



TITLE:

# Effective Bulk Activation and Interphase Stabilization of Silicon Negative Electrode by Lithium Pre-Doping for Next-Generation Batteries

AUTHOR(S):

Saito, Morihiro; Kato, Kiyomi; Ishii, Shunya; Yoshii, Kazuki; Shikano, Masahiro; Sakaebe, Hikari; Kiuchi, Hisao; Fukunaga, Toshiharu; Matsubara, Eiichiro

---

CITATION:

Saito, Morihiro ...[et al]. Effective Bulk Activation and Interphase Stabilization of Silicon Negative Electrode by Lithium Pre-Doping for Next-Generation Batteries. Journal of The Electrochemical Society 2019, 166(3): A5174-A5183

ISSUE DATE:

2019

URL:

<http://hdl.handle.net/2433/241728>

RIGHT:

© The Author(s) 2018. Published by ECS. This is an open access article distributed under the terms of the Creative Commons Attribution 4.0 License (CC BY, <http://creativecommons.org/licenses/by/4.0/>), which permits unrestricted reuse of the work in any medium, provided the original work is properly cited.



JES FOCUS ISSUE OF SELECTED PAPERS FROM IMLB 2018

# Effective Bulk Activation and Interphase Stabilization of Silicon Negative Electrode by Lithium Pre-Doping for Next-Generation Batteries

Morihiro Saito,<sup>1,\*</sup> Kiyomi Kato,<sup>1</sup> Shunya Ishii,<sup>1</sup> Kazuki Yoshii,<sup>2</sup> Masahiro Shikano,<sup>2</sup> Hikari Sakaebe,<sup>2,\*</sup> Hisao Kiuchi,<sup>3</sup> Toshiharu Fukunaga,<sup>3</sup> and Eiichiro Matsubara<sup>4</sup>

<sup>1</sup>Department of Applied Chemistry, Tokyo University of Agriculture and Technology, Koganei-shi, Tokyo 184-8588, Japan

<sup>2</sup>Research Institute of Electrochemical Energy, Department of Energy and Environment, National Institute of Advanced Industrial Science and Technology (AIST), Ikeda, Osaka 563-8577, Japan

<sup>3</sup>Office of Society-Academia Collaboration for Innovation, Kyoto University, Kyoto 611-0011, Japan

<sup>4</sup>Department of Materials Science and Engineering, Kyoto University, Kyoto 606-8501, Japan

To clarify the effects of Li pre-doping of a Si negative electrode for potential application in next-generation energy storage systems, such as Li-S and Li-O<sub>2</sub> batteries, such electrodes were prepared by direct Li pre-doping using Li metal foil and by electrochemical pre-doping at 700 mA g<sup>-1</sup> (Si) using a two-electrode cell. These were evaluated by comparing their charge/discharge properties, mainly by half-cell operation at a limited capacity of 2000 mAh g<sup>-1</sup> (Si). Fluoroethylene carbonate (FEC) was added to form a stable solid electrolyte interphase film on the surface of the electrodes. The depth and homogeneity of Li pre-doping were improved by using the direct Li pre-doping method and by FEC addition, respectively. The rapid Li pre-doping of this method caused cracks and pulverization of the Si nanoparticles and promoted deep Li alloying by decreasing the Li<sup>+</sup> diffusion distance. The tough homogeneous solid electrolyte interphase film derived from FEC suppressed electrolyte decomposition and enabled a fast Li alloying/de-alloying reaction. Addition of 10 mass% FEC to the half-cell electrolyte repaired damage to the interphase film caused by the large volume change of Si nanoparticles and improved cyclability to exceed 230 cycles.

© The Author(s) 2018. Published by ECS. This is an open access article distributed under the terms of the Creative Commons Attribution 4.0 License (CC BY, <http://creativecommons.org/licenses/by/4.0/>), which permits unrestricted reuse of the work in any medium, provided the original work is properly cited. [DOI: 10.1149/2.0271903jes]



Manuscript submitted October 22, 2018; revised manuscript received December 6, 2018. Published December 18, 2018. *This paper is part of the JES Focus Issue of Selected Papers from IMLB 2018.*

In recent years, new-generation energy storage systems, such as Li-S and Li-O<sub>2</sub> batteries, have attracted much attention because of the energy density limitations of Li-ion batteries.<sup>1</sup> These new-generation batteries have much higher energy densities, exceeding 500 Wh kg<sup>-1</sup>. These high-energy storage systems do not have the Li as the positive electrode and need to use Li metal as the negative electrode (NE), the theoretical capacity of which is 3860 mAh g<sup>-1</sup>. However, a Li metal NE risks short-circuiting by Li dendrite deposition and has poor rate capability because of its small surface area due to the flatness of the electrode, which typically takes the form of a foil or thin film. In contrast, Si is a good NE candidate for these batteries because of its high theoretical capacity (ca. 4200 mAh g<sup>-1</sup>)<sup>2,3</sup> and relative suppression of Li dendrite deposition by the charge/discharge process due to the Li alloying/de-alloying reactions. In addition, Si active materials usually use nano-materials, such as nanoparticles (NPs),<sup>4-11</sup> nano-wires,<sup>12-17</sup> and nano-flakes.<sup>18,19</sup> This not only suppresses fading of the capacity due to cracking and pulverization of Si active materials but also improves the cyclability and rate capability of Si NEs by increasing the reaction area.

To apply Si NEs to next-generation batteries, it is necessary to pre-dope them with Li, i.e., Li alloying. The development of easier and more convenient methods of pre-doping Li into Si NEs and detailed investigation of their resulting charge/discharge properties is important. Recent research on Li pre-doping into graphite and hard carbon NEs has been undertaken in study of Li-ion capacitors,<sup>20,21</sup> but there are very few reports of Li pre-doping of Si NEs.<sup>22,23</sup> We also previously prepared Li pre-doped Si NEs and tried to assemble Li-ion capacitors,<sup>24</sup> demonstrating stable operation to 800 cycles,<sup>25</sup> where their operating range was around 500 mAh g<sup>-1</sup> (Si). However, the influence of Li pre-doping on the electrochemical properties and their mechanism are still not sufficiently clarified especially at a larger operating range for next-generation batteries.

In this study, we prepared Li pre-doped Si NEs by direct Li pre-doping (DP) using Li metal foil and by electrochemical pre-doping (EP) using a two-electrode cell, both without and with fluoroethylene carbonate (FEC) as an additive to form a stable solid electrolyte interphase (SEI) film on the Si NE surface. The electrochemical data for the four Li pre-doped Si NEs were compared, mainly by half-cell operation at a limited capacity of 2000 mAh g<sup>-1</sup> (Si). Their charge/discharge properties and cyclability were investigated in detail from the viewpoints of Si bulk activation and interphase stabilization by proper SEI formation on the electrode surface. The charge/discharge properties of Li pre-doped Si NE using an FEC additive in both Li pre-doping and half-cell electrolytes were also evaluated.

## Experimental

**Preparation of nanosilicon-coated negative electrodes.**—Si NPs (Nanostructured & Amorphous Materials, Inc.; average particle size: 30–50 nm) were used as the Si active material. A slurry was prepared by mixing 80 mass% Si NPs, 5 mass% Ketjen Black (KB; Lion, EC600JD) as a conductive agent, and 15 mass% polyimide binder (I.S.T Corporation, Dream bond; solid ratio: ca. 46%) with N-methyl-2-pyrrolidone (NMP; Wako) as a solvent. The slurry was coated on Cu foil (Fukuda Metal Foil & Powder Co., Ltd.; thickness: 35 μm) as a current collector, dried at 60°C for 1 h, cured at 200°C for 12 h under vacuum, and then cut into circles (φ = 16 mm; i.e., the NE area was ca. 2 cm<sup>2</sup>). The thickness of the Si NE coating was ca. 6 μm, which corresponded to a loading mass of 0.45–0.57 mg (Si) cm<sup>-2</sup> as an active material. Li pre-doping and cell assembly were performed in an Ar-filled dry box (Miwa, MDB-1BK-NT1).

**Preparation of lithium pre-doped silicon negative electrodes.**—For Li pre-doping, two methods were used. In the DP method,<sup>24,25</sup> the Si NE was contacted with Li metal foil (Honjo Metal, thickness: 0.05 mm) and then immersed in 1.0 M LiPF<sub>6</sub> dissolved in ethylene carbonate and dimethyl carbonate (EC + DMC, 1:1 by volume; Tomiyama Pure Chemical Industries, Ltd., battery grade) at room

\*Electrochemical Society Member.

<sup>2</sup>E-mail: [mosaito@cc.tuat.ac.jp](mailto:mosaito@cc.tuat.ac.jp)

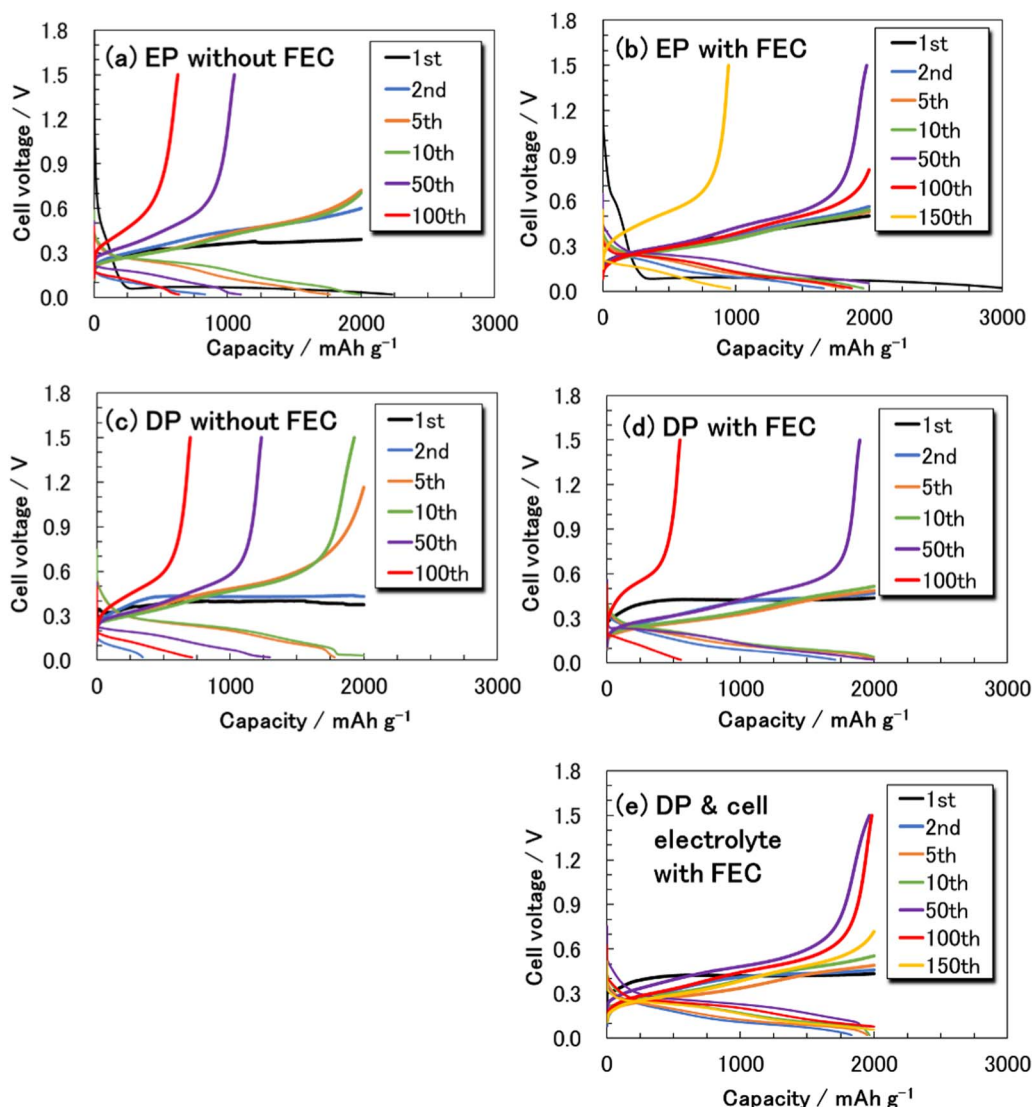


**Figure 1.** Charge/discharge curves of lithium pre-doped silicon negative electrode half-cells prepared using the (a, b) electrochemical pre-doping (EP) and (c, d, e) direct pre-doping (DP) methods.

temperature for 3 h. The EP method used a Si NE half-cell [Si NE | Li metal foil (Honjo Metal, thickness: 0.5 mm)] that was operated in constant-current mode at a rate of C/6 ( $700 \text{ mA g}^{-1}$ ) for the Si NPs from the open circuit potential to 0.02 V vs. Li/Li<sup>+</sup> using a battery test system (Hokuto Denko, HJ1001SM8). In some experiments, 10 mass% FEC (Kishida Chemicals, battery grade) was added to the electrolyte prior to Li pre-doping. A vacuum pressure impregnation treatment was conducted prior to Li pre-doping.

In this study, the Li pre-doped Si NEs by the DP and EP methods with the use and non-use of 10 mass% FEC additive were defined as “DP without FEC”, “DP with FEC”, “EP without FEC” and “EP with FEC”, respectively.

**Assembly of half-cells and electrochemical evaluation.**—Coin-type half-cells were constructed, using the Li pre-doped Si NEs as the working electrode, a separator (TEF4030, Nippon Kodoshi), and Li metal (Honjo metal, thickness: 0.5 mm) as the counter electrode, in the same dry box used for the Li pre-doping process, 1.0 M LiPF<sub>6</sub>/EC + DMC (1:1 by volume) without and with 10 mass% FEC was used as the electrolyte. Charge/discharge (Li alloying/de-alloying) tests were carried out in constant-current mode at C/6 ( $700 \text{ mA g}^{-1}$  (Si)) between 1.5 and 0.02 V using a battery test system (Hokuto Denko, HJ1001SM8). The charge/discharge ca-

capacity was limited to  $2000 \text{ mAh g}^{-1}$  (Si). Cyclic voltammetry (CV) was performed at a potential scanning rate of  $0.10 \text{ mV s}^{-1}$  between 1.50 and 0.02 V using an electrochemical measurement system (BioLogic Science Instruments, VSP). All measurements were conducted at 30°C.

For the “DP with FEC” electrode, we also subjected the charge/discharge test using 10 mass% FEC-added electrolyte to investigate the effect of FEC in the electrolyte by comparing with the “EP with FEC”. The data was defined as “DP & cell electrolyte with FEC”.

**Characterization of lithium pre-doped silicon negative electrodes.**—Morphology changes of the Si NEs before and after Li pre-doping were observed by scanning electron microscopy (SEM; JEOL, JSM-6510LA) using an accelerating voltage of 15 kV. The volume change of the Si NPs was evaluated by scanning probe microscopy (SPM; SHIMADZU, SPM-9700HT) in an Ar-filled glove box (Glovebox Japan Inc., GBJF100). The SPM imaging was conducted in phase mode, using a Si cantilever (NanoWorld Pointprobe NCH probes). The bulk crystal phases of the Si NPs were identified by X-ray diffraction (XRD; Rigaku, SmartLab) using Cu K $\alpha$  radiation (45 kV, 200 mA). The chemical components of SEI films formed on the surfaces of the Si NEs were analyzed by X-ray photoelectron

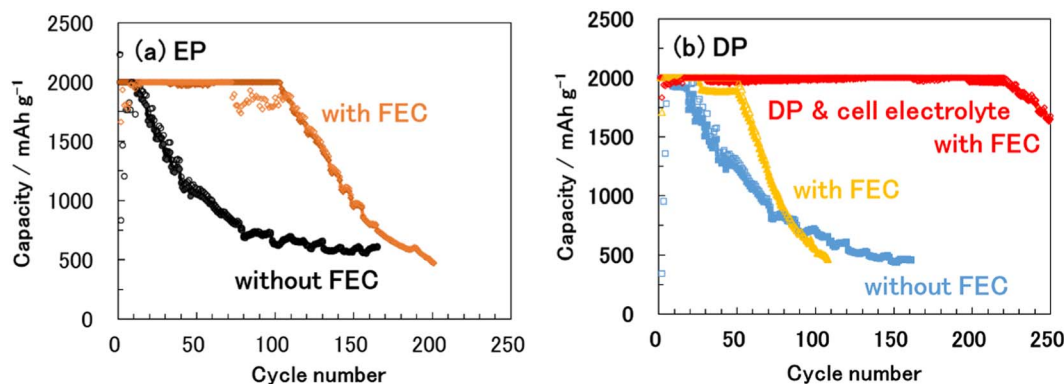


**Figure 2.** Cyclability of lithium pre-doped silicon negative electrode half-cells prepared using the (a) electrochemical pre-doping (EP) and (b) direct pre-doping (DP) methods.

spectroscopy (XPS; ULVAC-PHI, INC., PHI 5000 VersaProbe) and hard X-ray photoelectron spectroscopy (HAXPES; Spring-8/BL28XU). Before all characterizations, the Si NEs were washed twice with 3 mL dimethyl carbonate (DMC; Kishida Chemicals, battery grade) to remove residual electrolyte around the samples and dried for 1 h. Transfer vessels were used to avoid moisture and air exposure. For the HAXPES analysis, charge correction was conducted using the LiF peak and the strength was normalized relative to the total area of the HAXPES peak for each element.

## Results and Discussion

**Charge/discharge properties of lithium pre-doped silicon negative electrode half-cells at capacity limitation of 2000 mAh g<sup>-1</sup> (Si).**—Figure 1 shows the discharge/charge curves of Li pre-doped Si NE half-cells prepared by the EP and DP methods without and with 10 mass% FEC. For the EP method, the first charging (Li alloying) curve decreased rapidly at around 0.10 V and maintained a low potential, indicating that the crystalline phase of Si was destroyed and an amorphous Li<sub>x</sub>Si<sub>y</sub> phase formed.<sup>26</sup> As a result, the discharge curve exhibited a slope from 0.20 V, i.e. de-alloying from the amorphous Li<sub>x</sub>Si<sub>y</sub> phase. Cyclability was improved by the addition of FEC to the electrolyte. The limiting capacity of 2000 mAh g<sup>-1</sup> (Si) was maintained to around 100 cycles, as shown in Fig. 2.

In contrast, the first discharge curve for electrodes prepared by the DP method started from ca. 0.4 V and was relatively flat, indicating the occurrence of de-alloying by phase transfer from the Li<sub>15</sub>Si<sub>4</sub> crystalline phase to the Li<sub>x</sub>Si<sub>y</sub> amorphous phase.<sup>26</sup> The Li<sub>15</sub>Si<sub>4</sub> crystalline phase was formed by deep Li alloying above 3580 mAh g<sup>-1</sup>. The DP method therefore enabled more rapid Li pre-doping than the EP method.

The presence of FEC improved the cyclability up to about 50 cycles; however, capacity fading was confirmed thereafter; however, capacity fading was significantly suppressed by also adding 10 mass% FEC into the electrolyte for the DP-treated Si NE half-cell (Fig. 2). The high capacity of 2000 mAh g<sup>-1</sup> (Si) was maintained for over 230 cycles. This meant that FEC in the electrolyte repaired the SEI film that was damaged by expansion and shrinkage of Li–Si alloy NPs during the charge and discharge cycles, respectively.

**Effects of method of lithium pre-doping and fluoroethylene carbonate additive.**—Figure 3 shows the dQ/dV curves of Si NE half-cells prepared by Li pre-doping using the EP and DP methods without and with 10 mass% FEC additive. In the case of the EP method, phase transfer of Si from crystalline to amorphous phases was clearly defined by the sharp peaks at 0.06 V. After the first Li alloying, the de-alloying process started at around 0.20 V; however, additional noise currents appeared in the discharge curves at around 0.31 V, which indicated electrolyte decomposition. The current remained after 10 cycles for the half-cell without FEC addition. After adding FEC to the electrolyte

(Fig. 3b), the noise current was significantly reduced and reversibility of the charge/discharge curves improved.

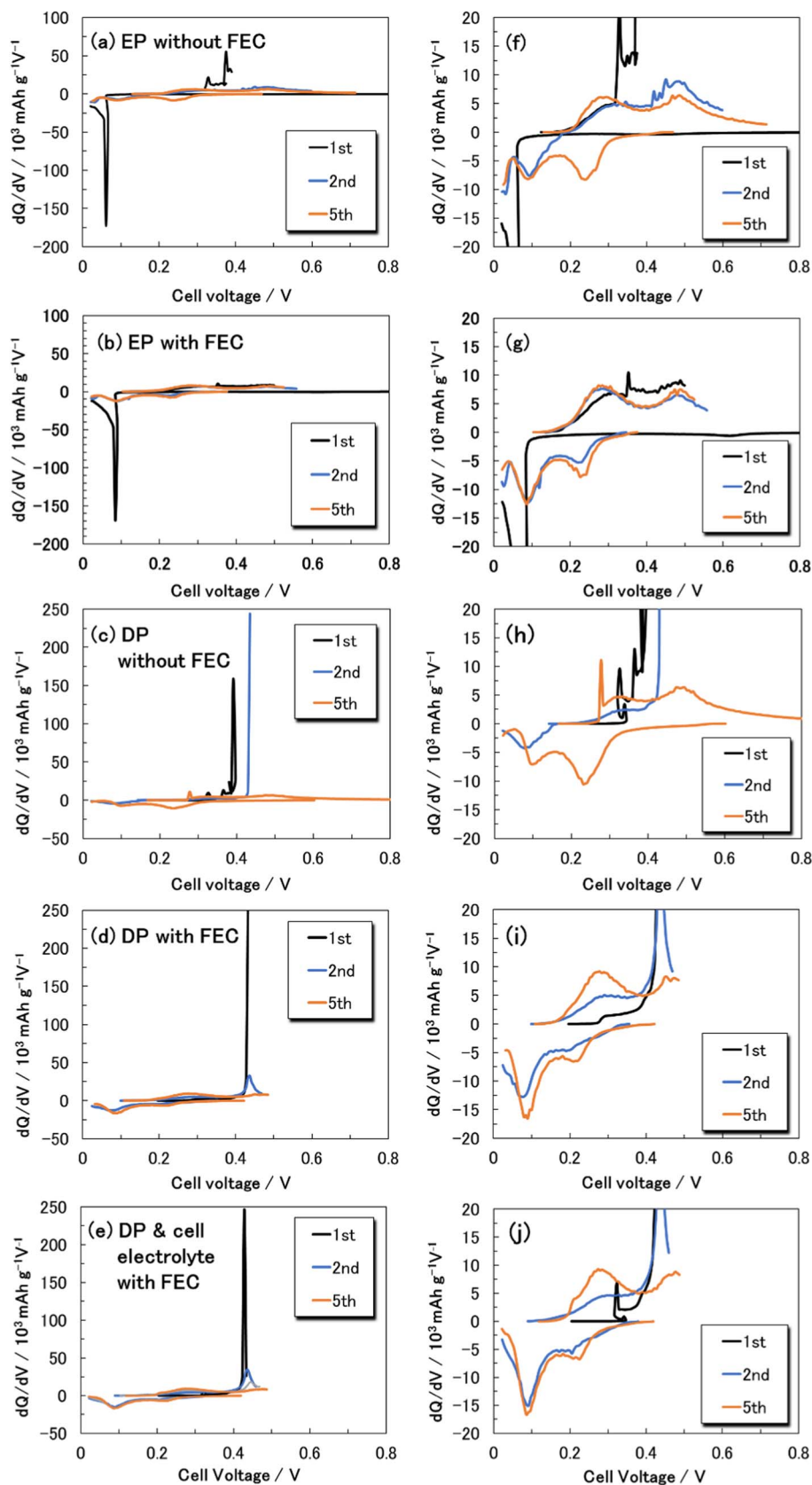
This behavior was confirmed for the DP-treated Si NE half-cells. Li pre-doped Si NE prepared by the DP method without FEC additive exhibited a similar noise current during the first discharge process at 0.32 V and during the following cycles at 0.27 V; however, the current due to electrolyte decomposition was clearly diminished by adding FEC to the electrolyte, thereby improving cyclability. Further addition of FEC to the half-cell electrolyte slightly increased the noise current. This indicated that the Si NPs were stabilized by growth of SEI film derived from the additional FEC additive in half-cell during initial cycles. In addition, all DP-treated Si NEs exhibited current peaks during the first discharge at around 0.4 V, which corresponded to de-alloying from Li<sub>15</sub>Si<sub>4</sub> to a Li<sub>x</sub>Si<sub>y</sub> amorphous phase. This implied that the DP method enabled much deeper Li pre-doping to be achieved than the EP method. As a result, the DP-treated Si NEs exhibited larger discharge/charge (de-alloying/alloying) currents including the following cycles. The FEC addition both at Li pre-doping and in half-cell electrolyte enhanced the effect and provided stability for the smooth de-alloying/alloying reaction.

**Homogeneity and depth of lithium pre-doping.**—From the electrochemical data for the Li pre-doped Si NEs, in particular that obtained by the DP method with addition of FEC, it was evident that Li pre-doping effectively influenced both the surface by formation of intact SEI films and the bulk structure of Si NPs. Figure 4 shows SEM images and insets of selected photographs of Li pre-doped Si NEs, both of which confirm the morphology changes. In the absence of FEC, Li pre-doping was inhomogeneous, i.e., part of the Si NE surface did not change to black (indicating more Li alloying) and the color remained gray (indicating less Li alloying) for both SEM and photographic images. In the gray region, many cracks caused by mechanical stress were observed, indicating inhomogeneity of Li alloying. For the EP method, the presence of a gas pool caused by electrolyte decomposition between the Si NE and separator after the Li pre-doping was confirmed: the gas prevented Li<sup>+</sup> supply to the Si NPs.

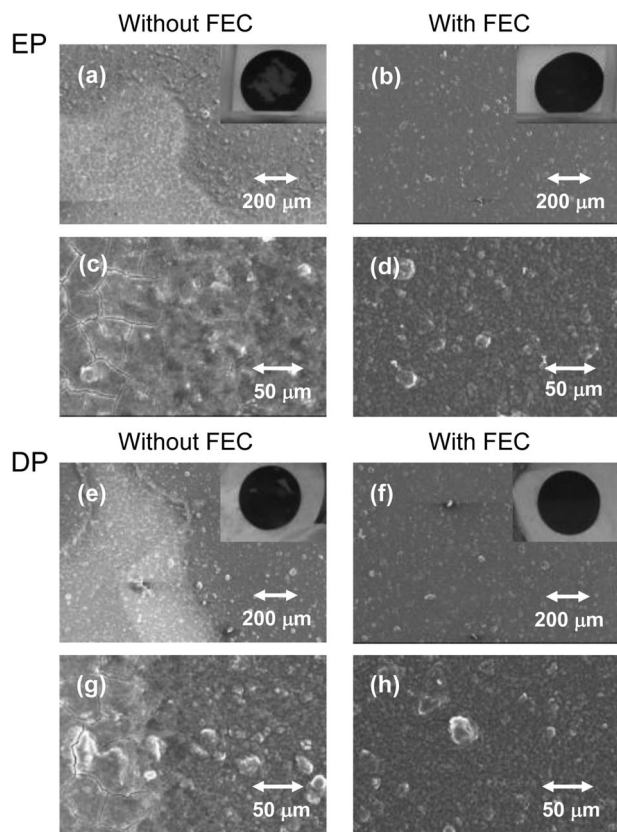
In contrast, Si NEs that used FEC in both the DP and EP methods clearly exhibited homogeneous Li alloying. This implied that FEC enabled homogeneous and coherent SEI films to form on the Si NE surface and suppressed some electrolyte decomposition that generated some of the gases. In particular, for the DP method, the black color of the Si NE images was deeper and aggregated Si NPs became larger, indicating deeper Li pre-doping. This is in good agreement with the trends of the charge/discharge properties, which indicated surface stabilization and sufficient bulk activation of Si NEs.

Figure 5 shows SPM images of Li pre-doped Si NEs. For those prepared using the EP method, the Si NPs gradually grew and their particle size increased with FEC addition. In contrast, the Si particle size was reduced by preparation using the DP method, implying





**Figure 3.**  $dQ/dV$  curves of lithium pre-doped silicon negative electrode half-cells prepared using the electrochemical pre-doping (EP) and direct pre-doping (DP) methods. (f), (g), (h), (i), and (j) are the expanded data toward y-axis of (a), (b), (c), (d), and (e), respectively.



**Figure 4.** Scanning electron micrographs of lithium pre-doped silicon negative electrodes prepared using the electrochemical pre-doping (EP) and direct pre-doping (DP) methods. (c), (d), (g), and (h) are the magnified images of (a), (b), (e), and (f), respectively.

cracking and pulverization of Si NPs by the rapid volume change caused by Li alloying. This also accelerated Li pre-doping and achieved deep homogeneous Li alloying.

**Lithium pre-doping rate and content.**—Figure 6a shows the first charging curves of Li pre-doped Si NE half-cells prepared by the EP method. The charge capacities were  $2233 \text{ mAh g}^{-1}$  and  $3021 \text{ mAh g}^{-1}$  without and with 10 mass% FEC, respectively. Although charge capacities included the irreversible capacities due to the electrolyte and FEC decomposition, they did not reach either the theoretical capacity (ca.  $4200 \text{ mAh g}^{-1}$ ) or the capacity for  $\text{Li}_{15}\text{Si}_4$  ( $3580 \text{ mAh g}^{-1}$ ), even though charging was increased by the FEC addition. From the first charging curve at around 0.60 V, the extra irreversible capacity due to FEC decomposition was  $< 100 \text{ mAh g}^{-1}$ ; therefore, the Li pre-doped content in the Si NE was considered to increase by addition of FEC to the electrolyte.

We also prepared two Si NE half-cells using the DP method without and with 10 mass% FEC and subjected these to external short-circuits. The currents obtained owing to the Li pre-doping are shown in Fig. 6b. The charge capacities were  $3338 \text{ mAh g}^{-1}$  and  $3885 \text{ mAh g}^{-1}$  without and with FEC, respectively. Both charge capacities were higher than those for electrodes prepared using the EP method, and the effect of FEC was confirmed. In addition, the DP method enabled rapid Li pre-doping and the charge capacities obtained after ca. 30 min exceeded those of electrodes prepared by the EP method. The DP method was therefore an effective way to achieve deep Li pre-doping in a short time. This was in good agreement with the decrease in Si particle size that occurred by cracking and pulverization due to the rapid volume change for the DP method. In particular, when adding FEC, the Li pre-doping rate was enhanced and the SEM observations (Fig. 4) showed that homogeneity also improved by formation of a proper SEI film on the Si NE surface.

Figure 7 shows XRD patterns of Li pre-doped Si NEs prepared using the two methods. For the EP method, the XRD peaks attributed to the Si crystalline phase at  $28^\circ$  and  $47^\circ$  remained, especially on non-addition of FEC. For the DP-treated Si NEs, these peaks became

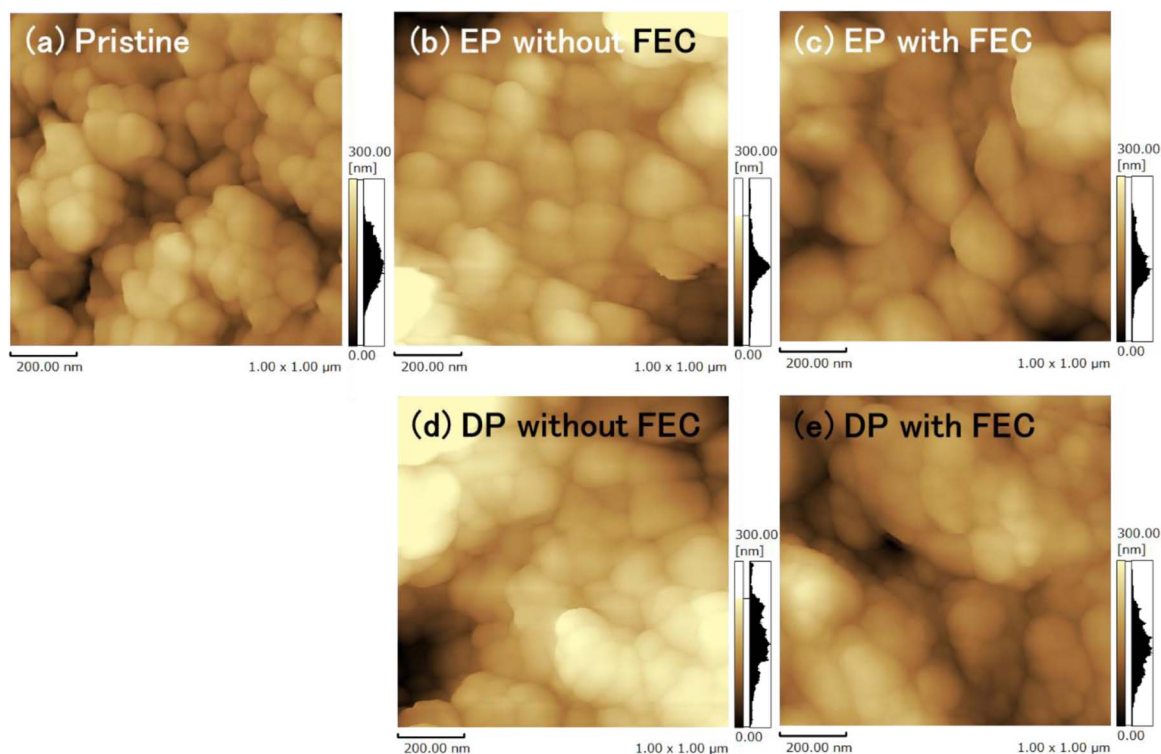


**Figure 5.** Scanning probe microscopy images of lithium pre-doped silicon negative electrodes prepared using the electrochemical pre-doping (EP) and direct pre-doping (DP) methods.

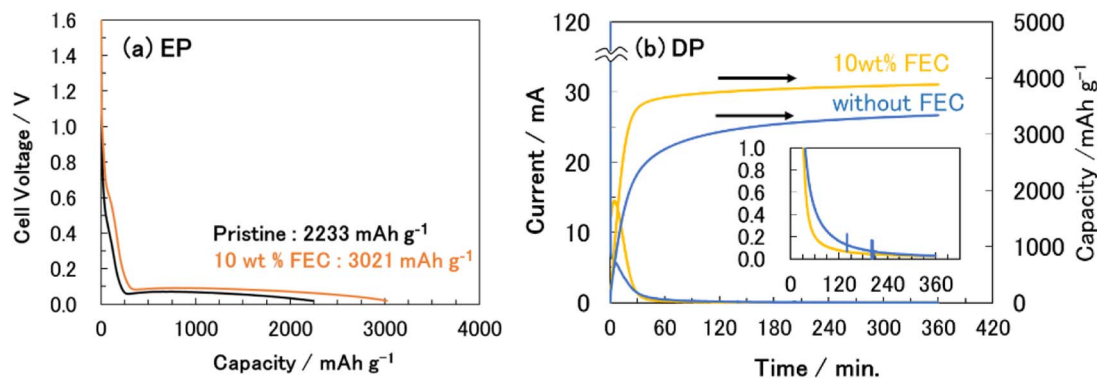


**Figure 6.** Charge curves and estimated Li contents for lithium pre-doping into silicon negative electrodes prepared using the electrochemical pre-doping (EP) and direct pre-doping (DP) methods. The detail of change in capacity is summarized Table S1.

quite small and those attributed to  $\text{Li}_{15}\text{Si}_4$  appeared at  $23^\circ$ ,  $26^\circ$ , and  $39^\circ$ , indicating deep Li pre-doping exceeding  $3580 \text{ mAh g}^{-1}$ .<sup>26</sup> The effect of FEC was also confirmed: peaks due to the crystalline phase of Si were completely diminished by preparation using the DP method with 10 mass% FEC.

**Effects of direct pre-doping method and fluoroethylene carbonate addition on Li alloying/de-alloying reaction.**—From the above results, it was evident that the DP method effectively increased the pre-doped Li content of all Si NPs by cracking and pulverization owing to rapid Li alloying. This increased their utilization ratio and enabled a fast Li alloying/de-alloying reaction. This effect was reflected by the reversibility of the charge/discharge reactions and  $dQ/dV$  curves. In summary, the DP method activated nano-crystalline Si-coated NE; however, these electrochemical data were limited to the applied capacity of  $2000 \text{ mAh g}^{-1}$  (Si).

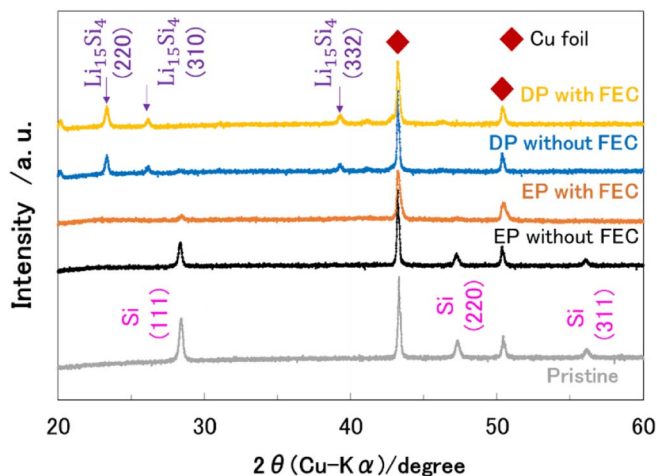
To more clearly determine the effects of this method and the presence of FEC on the electrochemical properties, CV curves were collected (Fig. 8). Initial enhancement of charge/discharge capacity was confirmed both without and with FEC additive, i.e., the activation effect was attributed to use of the DP method itself. In addition, curves generated in the absence of FEC exhibited a large and wide oxidation current owing to electrolyte decomposition from around 0.6 V, which continued until the following charging process, i.e., until formation of a new SEI film from  $< 0.4 \text{ V}$ . This was probably caused by the large volume change of Si NPs from  $\text{Li}_{15}\text{Si}_4$  crystalline to  $\text{Li}_x\text{Si}_y$  amorphous phases during the first discharge. The SEI film

that formed on the Si NE surface was not sufficiently stable against large volume changes. When using FEC, electrolyte decomposition was significantly suppressed by the stable SEI film and subsequent charge/discharge curves also improved. This indicated that the SEI film formed when using FEC was more stable and resistant to the large volume change of the Si NPs. This was more clearly observed by a further addition of 10 mass% FEC to the half-cell, which indicated that the extra FEC repaired the damage caused to the SEI film by the large volume changes during the charge/discharge cycles.

**Homogeneity and chemical composition of solid electrolyte interphase films.**—Figure 9 shows elasticity images of SEI films on the Li pre-doped Si NEs. In the absence of FEC, the elasticity distribution had two peaks; however, for both preparation methods, only one peak appeared after addition of FEC. This indicated that the SEI film became more homogeneous when derived from FEC and repaired properly in response to the smooth and fast Li alloying/de-alloying reaction for subsequent cycles. Viscoelastic images (Fig. S1) exhibited the same trend and were in good agreement with the high elasticity images, suggesting the formation of an organic polymer-based SEI film.

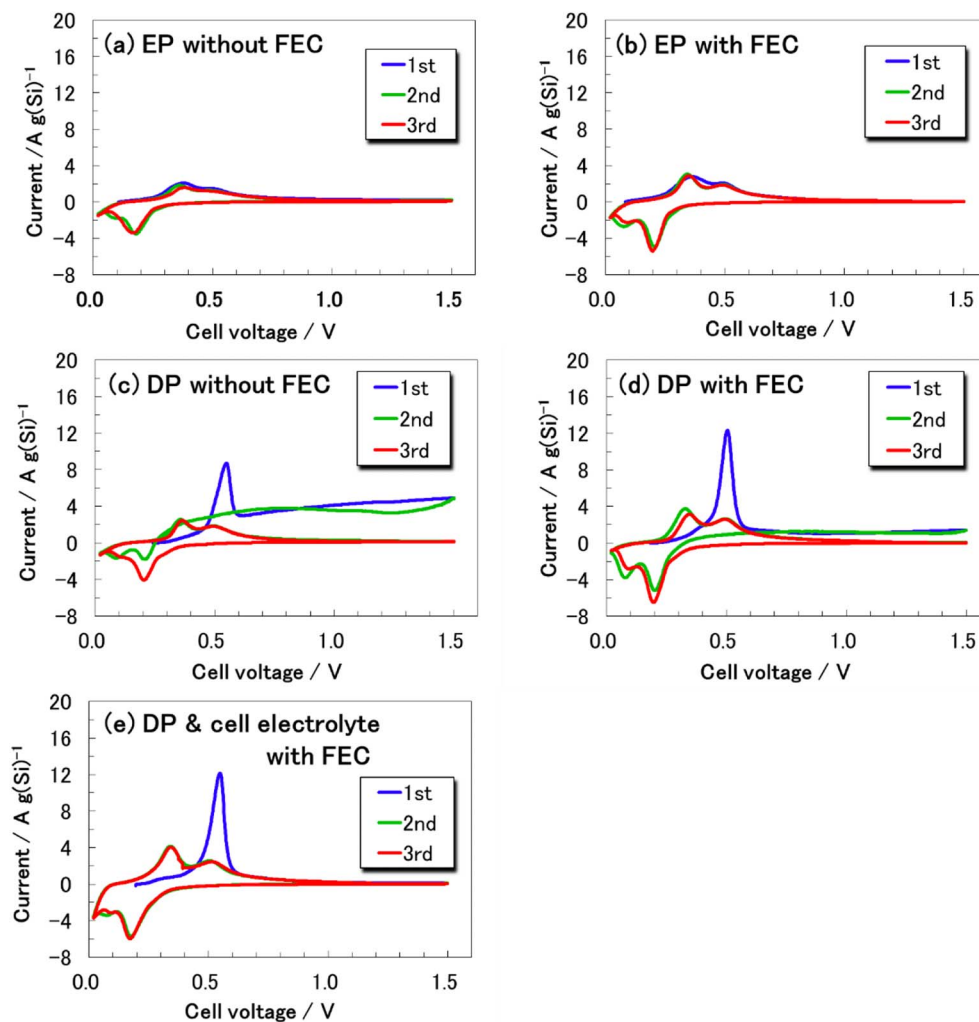
Differences in components of the SEI films derived from the two methods were investigated by XPS and HAXPES analyses. Figure 10 shows the XPS spectra: there was no significant difference between the two methods. Similar trends were confirmed for both methods with respect to FEC, i.e., SEI films that formed with FEC addition included an increase in C compounds, such as a more flexible polymeric layer and  $\text{Li}_2\text{CO}_3$ , that were derived from its decomposition. This is in good agreement with results reported by Veith et al.<sup>27</sup> In contrast, the XPS spectra due to LiF became smaller than those for electrodes prepared in the absence of FEC. This implied that DP-treated Si NE formed an organic polymer-rich condensed SEI film on the Si NP surfaces over a LiF-rich layer, i.e., the deeper Li pre-doping lowered the potential of the Si NPs, which enhanced FEC decomposition to form a stable layered SEI film, which made it tougher and more flexible. The surface of the SEI film formed in the absence of FEC was LiF-rich, indicating poor coverage of LiF by an organic polymer layer. The SEI film probably easily exfoliated from the Si NP surfaces due to the large volume change during the charge/discharge cycles. From this point of view, the DP method has an advantage over the EP method because of the lower potential of Li pre-doping: the C 1s peak due to the organic polymer layer increased and the F 1s peak due to LiF decreased when compared with those of the EP method. Use of the DP method is therefore considered to give a tougher and more flexible SEI film.

Figure 11 shows HAXPES data for the Li pre-doped Si NEs. The DP method and FEC addition were found to effectively destroy the Si crystalline phase and convert it to an amorphous phase. In addition, the DP-treated Si NEs exhibited a  $\text{SiO}_x\text{F}_y$  phase<sup>28,29</sup> on the Si NPs. This indicated that rapid and strong Li pre-doping enabled surface fluorination of the Si NPs. DP-treated Si NEs are suggested to be



**Figure 7.** X-ray diffraction patterns of lithium pre-doped silicon negative electrodes prepared using the electrochemical pre-doping (EP) and direct pre-doping (DP) methods.





**Figure 8.** Cyclic voltammograms of lithium pre-doped silicon negative electrodes prepared by the direct pre-doping (DP) method without and with the addition of fluoroethylene carbonate (FEC).

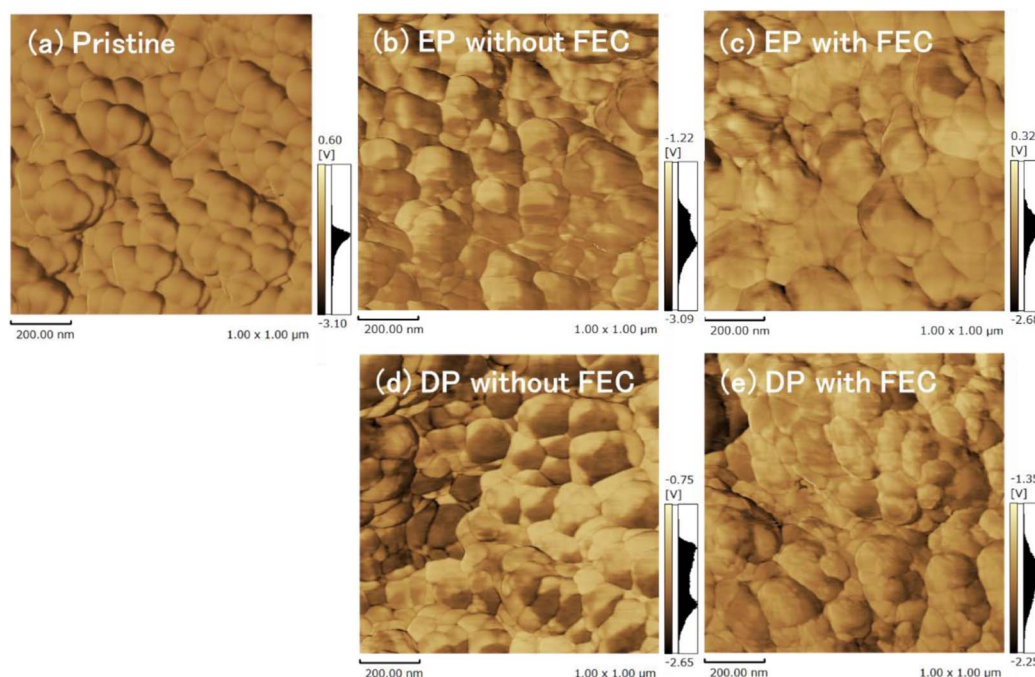


**Figure 9.** Elasticity images of lithium pre-doped silicon negative electrodes prepared by the electrochemical pre-doping (EP) and direct pre-doping (DP) methods.



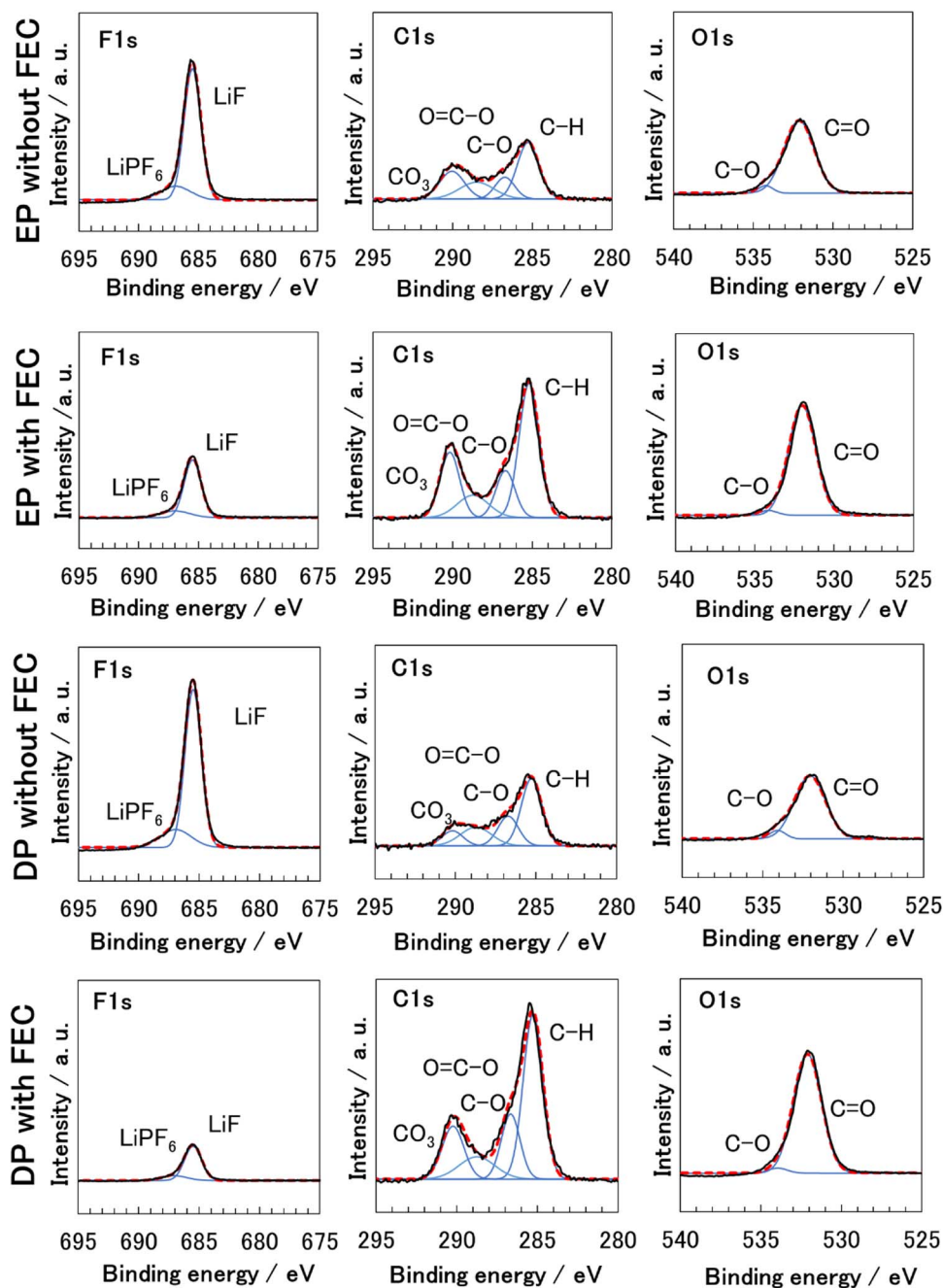


**Figure 10.** X-ray photoelectron spectra of lithium pre-doped silicon negative electrodes prepared using the electrochemical pre-doping (EP) and direct pre-doping (DP) methods.

protected by triple-layered SEI films on the Si NP surfaces, i.e., an inorganic layer consisting of  $\text{SiO}_x\text{F}_y$  and  $\text{Li}_x\text{SiO}_y$ , a LiF-rich layer, and a tough, flexible organic polymer layer.

**Mechanism of silicon interphase stabilization by direct pre-doping method.**—Figure 12 shows schematic models of the Li pre-doped Si NEs prepared by the two methods without and with FEC. For the EP method without FEC, the initially formed SEI film was not homogeneous or tough, which caused the capacity to fade by continuous electrolyte decomposition during subsequent charge/discharge cycling; however, FEC addition changed the chemical composition and homogeneity of the SEI film and increased the Li content in the Si NEs.

When using the DP method with FEC, the effects were maintained and deeper Li pre-doping was achieved. This increased the organic polymer layer on the LiF-rich layer in the SEI film and partially fluorinated the surface of the Si NPs. The resulting three-layered structure gave excellent toughness and flexibility against the volume change of Si NPs.

Combination of the DP method and FEC addition therefore achieved bulk activation and stabilized the interphase of the Si NPs. FEC addition was effective in improving the cyclability of Si NEs; however, for DP-treated Si NEs, the volume change between the  $\text{Li}_{15}\text{Si}_4$  and  $\text{Li}_x\text{Si}_y$  amorphous phases was severe, which caused damage to the SEI film. Further FEC addition into the half-cell electrolyte was useful to repair the weaker and damaged points to maintain good cyclability.

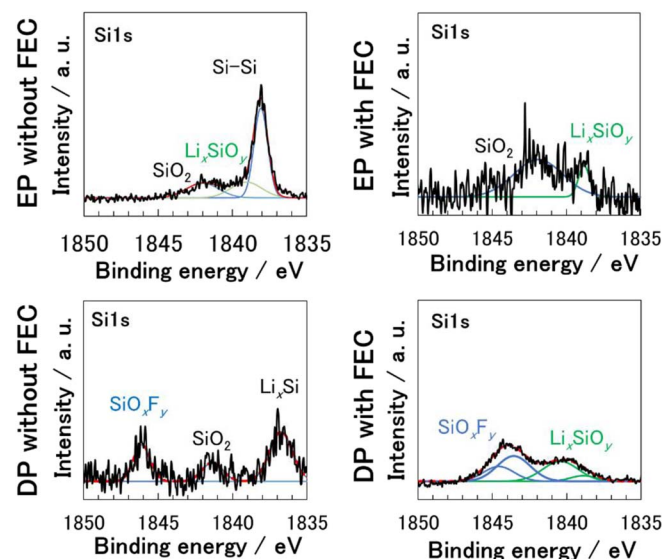


**Figure 11.** Hard X-ray photoemission spectra of lithium pre-doped silicon negative electrodes prepared using the electrochemical pre-doping (EP) and direct pre-doping (DP) methods. Data for other elements are summarized in Fig. S2.

## Conclusions

Li pre-doping of Si NEs using the EP and DP methods and their charge/discharge properties were investigated for application to next-generation batteries. For both methods, addition of FEC was effective in improving homogeneity and deepening Li pre-doping. The DP method enabled a further increase of the Li content by more rapid Li pre-doping; however, the deep Li pre-doping damaged the SEI film during the discharge process (Li de-alloying from the  $\text{Li}_{15}\text{Si}_4$  crystalline phase) and resulted in fading capacity. Further addition of FEC to the half-cell electrolyte repaired the damaged SEI film and improved cyclability. Combination of the DP method and FEC

addition enabled cyclability to be improved to exceed 230 cycles at the capacity limitation of  $2000 \text{ mAh g}^{-1}$  (Si).

The key points from this study are as follows: i) use of the DP method, compared with the EP method, enabled deeper Li pre-doping by pulverization of Si nanoparticles owing to rapid Li alloying; ii) FEC addition in the DP method improved the chemical composition and homogeneity of the SEI film, which improved its toughness and flexibility by increasing the organic polymer layer on the LiF-rich layer in the film; iii) further addition of FEC to the half-cell electrolyte repaired damaged parts of SEI film attributed to the large volume change of Si NE.

Per the above results, after Li pre-doping, the Si NE should be operated below at least  $3580 \text{ mAh g}^{-1}$ , corresponding to the formation of the  $\text{Li}_{15}\text{Si}_4$  crystalline phase; however, this specific capacity is still attractive as an alternative to the Li metal NE (ca.  $3800 \text{ mAh g}^{-1}$ ). The Li metal NE is generally considered for use at half dissolution and half deposition, corresponding to ca.  $1900 \text{ mAh g}^{-1}$  (Li); therefore, the capacity limitation of  $2000 \text{ mAh g}^{-1}$  (Si) is not too small to apply to next-generation batteries. Further studies of the charge/discharge process at a capacity limitation of  $3000 \text{ mAh g}^{-1}$  (Si) are now in progress to more clearly elucidate the influence and effect of Li pre-doping to Si NE.

## Acknowledgments

This work was partially supported by the New Energy and Industrial Technology Development Organization (NEDO) Project for the Research and Development Initiative for Scientific Innovation of New Generation Batteries 2 (RISING 2), the Ministry of Education, Culture, Sports, Science and Technology (MEXT) Program for the Development of Environmental Technology using Nanotechnology, and a Scientific Technology Human Resource Development grant, Japan. The synchrotron radiation experiments were performed at the BL28XU in SPring-8 with the approval of the Japan Synchrotron Radiation Research Institute (JASRI) (Proposal Nos. 2017B7610 and 2018A7610).

## ORCID

Morihiro Saito  <https://orcid.org/0000-0001-7062-8336>

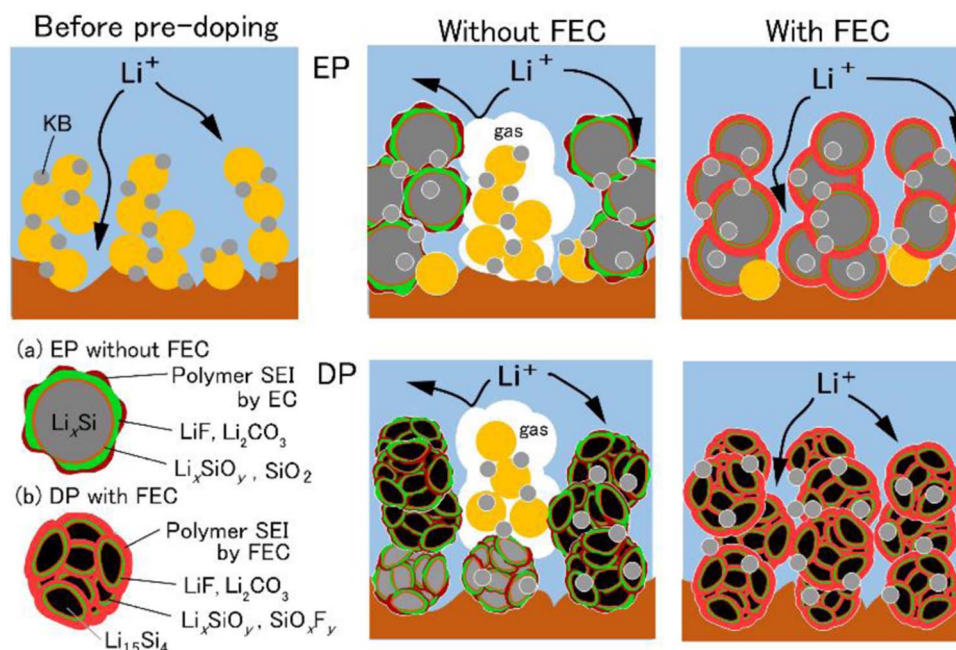


**Figure 12.** Schematic models of lithium pre-doped silicon negative electrodes prepared using the electrochemical pre-doping (EP) and direct pre-doping (DP) methods.

Kazuki Yoshii  <https://orcid.org/0000-0001-8904-6790>  
Masahiro Shikano  <https://orcid.org/0000-0002-8710-9759>

## References

1. P. G. Bruce, S. A. Freunberger, L. J. Hardwick, and J. M. Tarascon, *Nat. Mater.*, **11**, 19 (2011).
2. R. A. Huggins, *J. Power Sources*, **81–82**, 13 (1999).
3. B. A. Boukamp, G. C. Lesh, and R. A. Huggins, *J. Electrochem. Soc.*, **128**, 725 (1981).
4. H. Li, X. Huang, L. Chen, Z. Wu, and Y. A. Liang, *Electrochem. Solid-State Lett.*, **2**(11), 547 (1999).
5. J. Yang, B. F. Wang, K. Wang, Y. Liu, J. Y. Xie, and Z. S. Wen, *Solid-State Lett.*, **6**(8), A154 (2003).
6. U. Kasavajjula, C. Wang, and A. J. Appleby, *J. Power Sources*, **163**, 1003 (2007).
7. H. Kim, M. Seo, M.-H. Park, and J. A. Cho, *Angew. Chem. Int. Ed.*, **49**, 2146 (2010).
8. J. Yang, Y. Takeda, N. Imanishi, C. Capiglia, J. Y. Xie, and O. Yamamoto, *Solid State Ionics*, **152–153**, 125 (2002).
9. T. Morita and N. Takami, *J. Electrochem. Soc.*, **153**(2), A425 (2006).
10. Y.-S. Hu, R. Demir-Cakan, M.-M. Tittrici, J.-O. Müller, R. Schlögl, M. Antonietti, and J. Maier, *Angew. Chem. Int. Ed.*, **47**(9), 1645 (2008).
11. C.-M. Park, W. Choi, Y. Hwa, J.-H. Kim, G. Jeong, and H.-J. Sohn, *J. Mater. Chem.*, **20**, 4854 (2010).
12. H. Kim and J. Cho, *Nano Lett.*, **8**, 3688 (2008).
13. L.-F. Cui, Y. Yang, C.-M. Hsu, and Y. Cui, *Nano Lett.*, **9**(9), 3370 (2009).
14. C. K. Chan, H. Peng, G. Liu, K. McIlwrath, X. F. Zhang, R. A. Huggins, and Y. Cui, *Nat. Nanotechnol.*, **3**, 31 (2008).
15. L.-F. Cui, R. Ruffo, C. K. Chan, H. Peng, and Y. Cui, *Nano Lett.*, **9**, 491 (2009).
16. C. K. Chan, R. Ruffo, S. S. Hong, R. A. Huggins, and Y. Cui, *J. Power Sources*, **189**, 34 (2009).
17. X. Chen, K. Gerasopoulos, J. Guo, A. Brown, C. Wang, R. Ghodssi, and J. N. Culver, *ACS Nano*, **4**(9), 5366 (2010).
18. K. Nakai, I. Tsuchioka, M. Saito, A. Tasaka, T. Takenaka, M. Hirota, A. Kamei, and M. Inaba, *Electrochemistry*, **78**(5), 438 (2010).
19. M. Saito, T. Yamada, C. Yodoya, A. Kamei, M. Hirota, T. Takenaka, A. Tasaka, and M. Inaba, *Solid State Ionics*, **225**, 506 (2012).
20. S. R. Sivakkumar and A. G. Pandolfo, *Electrochim. Acta*, **65**, 280 (2012).
21. W. J. Cao and J. P. Zheng, *J. Electrochem. Soc.*, **160**(9), A1572 (2013).
22. T. Okubo, M. Saito, C. Yodoya, A. Kamei, M. Hirota, T. Takenaka, T. Okumura, A. Tasaka, and M. Inaba, *Solid State Ionics*, **262**, 39 (2014).
23. Y. Domi, H. Usui, D. Iwanari, and H. Sakaguchi, *J. Electrochem. Soc.*, **164**(7), A1651 (2017).
24. M. Saito, K. Takahashi, K. Ueno, and S. Seki, *J. Electrochem. Soc.*, **163**(14), A3140 (2016).
25. M. Saito, M. Osawa, A. Masuya, and K. Kawakatsu, *Electrochemistry*, **85**(10), 656 (2017).
26. J. Li and J. R. Dahn, *J. Electrochem. Soc.*, **154**(3), A156 (2007).
27. G. M. Veith, M. Doucet, R. L. Sacci, B. Vacaliuc, J. K. Baldwin, and J. F. Browning, *Sci. Rep.*, **7**, 6326 (2017).
28. B. T. Young, D. R. Heskest, C. C. Nguyen, M. Nie, and J. C. Woicik, *ACS Appl. Mater. Interfaces*, **7**, 20004 (2015).
29. F. Jeschull, F. Lindgren, M. J. Lacey, F. Björefors, K. Edström, and D. Brandell, *J. Power Sources*, **325**, 513 (2016).